Title	In situ study of growth mechanism of germanene segregated through Ag(111) thin films by Raman and X-ray photoelectron spectroscopy
Author(s)	Tomo-o Terasawa, Daiki Katsube, Masahiro Yano, Takahiro Ozawa, Yasutaka Tsuda, Akitaka Yoshigoe, Hidehito Asaoka, and Seiya Suzuki
Citation	Chemistry of Materials, 38,6,p. 2933 - 2945
Text Version	Submitted Manuscript
URL	https://jopss.jaea.go.jp/search/servlet/search?5087395
DOI	https://doi.org/10.1021/acs.chemmater.5c03462
Right	This document is the unedited Author's version of a Submitted Manuscript subsequently accepted for publication in Chemistry of Materials, copyright © 2026 American Chemical Society. To access the final published article, see ACS Articles on Request.

In situ study of growth mechanism of germanene segregated through Ag(111) thin films by Raman and X-ray photoelectron spectroscopy

*Tomo-o Terasawa[1, 2, *], Daiki Katsube[3], Masahiro Yano[1], Takahiro Ozawa[2], Yasutaka Tsuda[1], Akitaka Yoshigoe[1], Hidehito Asaoka[1], and Seiya Suzuki[1].*

[1]Japan Atomic Energy Agency, [2]The University of Tokyo, [3]Japan Fine Ceramics Center,

Germanene, a honeycomb lattice of Ge atoms, has attracted attention for next-generation electronics and as a topological material. Among reported synthesis routes, the segregation method enables reproducible monolayer germanene formation on Ag(111) through simply annealing an Ag(111) thin film on a Ge(111) substrate. Despite this success, the physical origins of its monolayer selectivity and the mechanism for suppressing competing Ge phases remain unclear. Here, we investigate germanene formation via Ge segregation using in situ Raman spectroscopy and X-ray photoelectron spectroscopy to directly track Ge behavior during annealing and cooling. In situ observations revealed that annealing at 500 °C yielded no Ge-related byproducts, and the system reached a high-temperature surface equilibrium state, independent of the initial Ge amount. Cooling from this state produced a Ge-enriched surface that stabilizes the formation of monolayer germanene. In contrast, heating only to 300 °C produced three-dimensional Ge islands without Ge-enrichment, followed by Ge–Ag alloy formation upon subsequent cooling. By integrating the

temperature-dependent diffusion length and the process-dependent diffusion direction, we established a unified description of Ge behavior on Ag/Ge(111) substrates, in which cooling-induced Ge-enrichment at the surface reproducibly stabilizes the selective formation of monolayer germanene.

INTRODUCTION

Germanene, a two-dimensional honeycomb lattice composed of monolayer Ge atoms, has attracted significant attention for its linear band dispersion together with a finite band gap of 24 meV [1,2], and its predicted topological nature, suggesting room temperature (RT) qubits hosting [3,4]. These features position germanene as a potential key material in next-generation electronics and quantum technologies.

Germanene has been successfully grown on various substrates, including Ag(111)[5–12], Au(111)[13–15], Cu(111)[16], Al(111)[17–20], Pt(111)[21], Ag-Al alloy[22], MoS_2[23], graphite[24], and Ge_2Pt alloy[25]. Among them, only germanene on Ag(111) and Au(111) exhibits vibrational signatures of Ge-Ge covalent bonding[7,11,15]. In addition, germanene on Ag(111) shows larger superstructures than those on Au(111)[6,9,15], which indicates better long-range order. They suggest that Ag(111) is the most effective substrate reported so far for high-quality germanene growth.

To date, most Ge-on-Ag(111) studies have used Ge deposition. Early works found the formation of surface alloys, Ag_2Ge[26–28]. By precisely controlling the Ge dose and growth rate, the growth of germanene was achieved[5]. More recently, Zhang et al. reported that Ge deposition below 200 °C yields a long-range ordered superstructure of $\sqrt{109} \times \sqrt{109}$ germanene[9]. However, they also reported the imperfect Ge lattice partially substituted by Ag[9].

Alternatively, Yuhara et al. demonstrated a segregation method in which, during annealing at 500 °C, Ge atoms diffuse through an Ag(111) thin film deposited on a Ge(111) substrate and form germanene on the surface by subsequent cooling[6]. A large-area, commensurate $7\sqrt{7} \times 7\sqrt{7}$ germanene was obtained in a monolayer form using this method[6]. In addition, germanene is easily oxidized but can be recovered by simple vacuum annealing[29], which is another advantage of the segregation method. Thus, brushing up on this method is beneficial as a future scalable growth technology for germanene applications.

However, the underlying mechanism of reproducible monolayer germanene formation via the segregation method remains unclear. It is still unknown how monolayer germanene selectively and stably forms, instead of Ge-related byproducts such as three-dimensional (3D) Ge islands and Ag_2Ge surface alloy[10,11]. Moreover, as germanene is considered a metastable state[30], clarifying how it is stabilized and under what thermal conditions it emerges, are essential for the further application of segregated germanene. Experimental investigations are further constrained by the oxidative instability of germanene, which necessitates in situ characterization at high temperatures (HTs) without breaking the vacuum.

In this study, we investigated the germanene formation through Ge segregation, employing in situ Raman spectroscopy and X-ray photoelectron spectroscopy (XPS) throughout the growth process. To clarify the behavior of Ge systematically, we prepared three types of samples with different initial amounts of Ge adsorbed on the surface and dissolved in the Ag thin film. Raman spectroscopy tracked the temperature evolution of Ge-Ge covalent bonds, elucidating the process by which germanene and its byproducts form. XPS revealed the amount and chemical states of surface Ge before and after germanene formation. In particular, in situ observations were

conducted at various temperatures not only during annealing but also during cooling, as germanene formation was observed upon cooling in this study.

By correlating the temperature-dependent behavior of Ge with its solubility and diffusion in Ag, we aim to clarify the conditions that lead to reproducible and selective monolayer formation of germanene rather than Ge byproducts. The underlying mechanism proposed here would provide a framework for understanding not only germanene growth via segregation but also via deposition, offering insights applicable to the segregation-driven synthesis of other 2D materials.

EXPERIMENTAL SECTION

Sample preparation. Three types of samples were prepared and referred to as pristine, germanene, and sputtered substrates (Figure 1a). These samples have different initial amounts of surface Ge and Ge dissolved in the Ag film. First, a Ge(111) substrate was cleaned by repeated Ar^+ sputtering and annealing, followed by deposition of a 150-nm-thick Ag film in a vacuum chamber with the base pressure of 3×10^{-8} Pa. After transferring into another vacuum chamber, the surface was further cleaned by 1 keV Ar^+ sputtering for 20 minutes before the experiments. This sample, referred to as the "pristine substrate," is used in XPS experiments. Second, germanene was grown by annealing the pristine substrate at 500 °C for 10 minutes and cooling to RT. The formation of germanene was confirmed by low-energy electron diffraction (LEED) using ErLEED (SPECS) at beam energies of 15 to 120 eV, as shown in Figures 1b, c. This sample is referred to as the "germanene substrate". Third, the germanene substrate was sputtered with Ar^+ for 10 minutes to remove the germanene layer, referred to as the "sputtered substrate". Removal of Ge was verified by XPS (Figure 3d). In summary, the pristine substrate contains no Ge either within or on the Ag film; the germanene substrate contains Ge both in and on the film; and the sputtered substrate

retains Ge only within the Ag thin film. Using these samples, we investigated how the initial Ge distribution influences germanene growth.

Experimental procedures. To investigate the growth mechanism of germanene, we performed in situ measurements along two types of thermal histories, hereafter referred to as "annealing" and "cooling" (Figures 1d, e). In the annealing experiment (Figure 1d), the sample was annealed at the designated HTs for at least 10 minutes, and Raman spectroscopy and XPS were performed (in separate experiments under identical annealing protocols) at the corresponding annealing temperatures. Subsequently, after decreasing the temperature to RT, the same technique (Raman spectroscopy or XPS) was performed again at RT. In the cooling experiments (Figure 1e), the temperature was increased to 500 °C and then decreased to designated intermediate temperatures (T_{interm}), at which Raman spectroscopy or XPS was performed. Then, the cooling was continued to RT, and the same technique (Raman spectroscopy or XPS) was performed at RT. The dynamics of Ge segregation and germanene formation were analyzed by varying the T_{interm}.

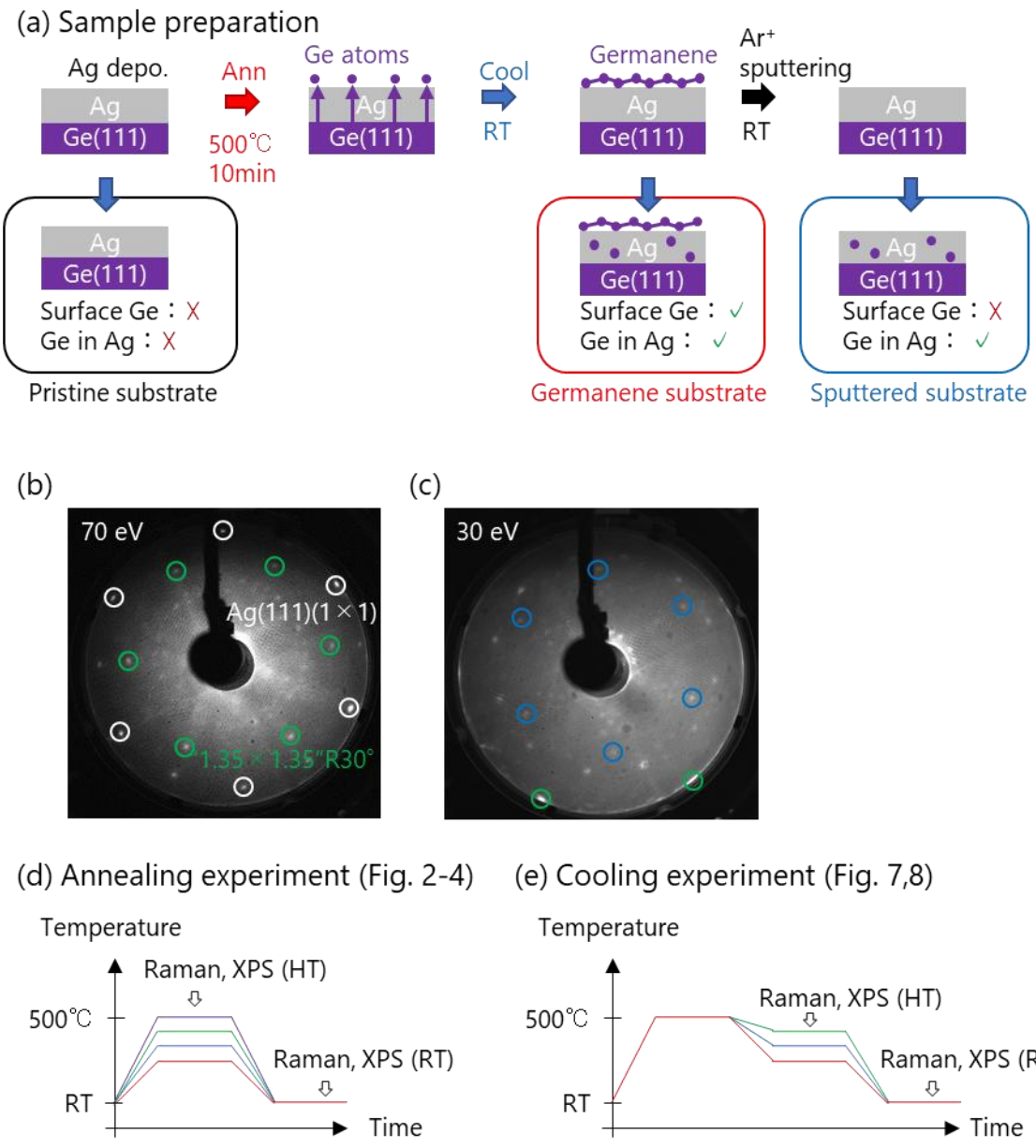

Figure 1. (a) Schematic illustration of sample preparation. (b, c) LEED patterns of germanene formed after annealing at 500 °C, observed at RT with electron beam energies of (b) 70 eV and (c) 30 eV. White, green, and blue circles highlight the Ag(111)(1 × 1), germanene, and other spots, following the same convention that Yuhara et al. reported[6]. (d, e) Temperature diagrams of annealing and cooling experiments, respectively.

Raman spectroscopy. We performed in situ Raman spectroscopy in a vacuum chamber (1×10^{-6} Pa). A 473 nm laser was incident at 60° to the surface normal for 10 minutes. The in situ experiments were performed using a home-built automatic system equipped with a direct current flow controller for an indirect heater composed of a Si plate. A pyrometer was used to monitor the substrate temperature. Concurrently, optical microscope images were acquired using a CMOS camera to avoid laser focusing on large 3D Ge islands. Note that, since oxygen exposure, even at a pressure of 5×10^{-6} Pa for 30 minutes, causes negligible O adsorption on germanene in our previous study[29], the present base pressure was sufficiently low to prevent oxidation of germanene during the experiments over several hours. Details of the chamber and microscope setup are provided elsewhere[31,32].

Synchrotron radiation XPS. We performed in situ XPS at BL23SU in SPring-8[29], using a surface reaction analysis apparatus (SUREAC2000) under ultrahigh vacuum (2×10^{-8} Pa). The incident photon energy was 700 eV, calibrated using the Fermi energy and the 4f peaks of Au. The incident angle was 30° from the surface normal, while the photoelectron escape angle was along the surface normal. For each experiment, survey spectra, as well as Ge 3d, Ag 3d, O 1s, C 1s, and valence band spectra, were recorded. We confirmed minimal contamination on the three substrates based on the O 1s and C 1s spectra (Figure S1). The sample temperature was measured with a thermocouple calibrated by the same pyrometer used in the Raman experiments. Ge 3d peaks were fitted using Voigt functions with one or two components (Figure S2), each consisting of the two spin-orbit peaks, Ge $3d_{5/2}$ and $3d_{3/2}$, with a spin-orbit splitting of 0.55 eV.

RESULTS

Annealing experiments. To examine the growth mechanism of germanene, it is critical to determine whether the Ge-Ge bonding exhibits germanene-like characteristics at each temperature. We thus performed in situ Raman spectroscopy to investigate the temperature dependence of Ge-Ge bonding (Figure 2a), using sputtered and germanene substrates to evaluate the influence of initial Ge amount on the Ag film. Typical Raman spectra of the sputtered (Figures 2b, c) and germanene (Figures 2d, e) substrates are presented, with Figures 2b, d at HTs and Figures 2c, e at RT.

For sputtered substrates at HTs (Figure 2b), a sharp peak at 300 cm^{-1} with a full width at half maximum (FWHM) of approximately 8 cm^{-1} appeared at 300 and 400 °C. The FWHM and peak position indicate sp^3-bonded Ge atoms[27,33] in 3D Ge islands[10,11]. Note that Ag_2Ge shows no Raman peaks in this spectral region[27]. The 300 cm^{-1} peak disappeared at 500 °C (Figure 2b), suggesting the instability of 3D Ge islands on Ag(111) at this temperature, which is also confirmed by optical microscopy (Figure S3). Whether this disappearance is due to Ge desorption or transformation into a different state will be elucidated later in Figure 3. After the subsequent cooling to RT from 500 °C (Figure 2c), germanene formation was observed, as evidenced by broad Raman peaks at ~156 and ~254 cm^{-1} assigned to the out-of-plane (oTO) and in-plane transverse optical (iTO) phonon modes of germanene, respectively[7,11]. In contrast, the peak near 300 cm^{-1} persisted after annealing at 300 and 400 °C and cooling to RT. Thus, germanene formation requires annealing at 500 °C, whereas lower annealing temperatures result in the 3D Ge island formation.

For germanene substrates at HTs (Figure 2d), germanene peaks were originally observed at around 150 and 260 cm^{-1} up to 200 °C. These peaks disappeared at 300–400 °C, and a peak corresponding to 3D Ge islands emerged instead. These 3D Ge islands also disappeared at 500 °C, similar to those on the sputtered substrate. After cooling to RT from 200–400 °C (Figure 2e), the

Raman spectral features at HT (Figure 2d) were preserved. After annealing at 500 °C followed by cooling to RT, germanene peaks reappeared, as observed for the sputtered substrate (Figure 2c). These results indicate that, regardless of the initial Ge amount on the Ag film, annealing at 500 °C followed by cooling leads to the formation of germanene.

Combining the results of sputtered and germanene substrates, the in situ Raman data in Figure 2 clarified how the Ge bonding states on the Ag(111) surface vary with temperature. From RT to 200 °C, the Ge bonding states remained unchanged. In the 300–400 °C range, Ge tends to form 3D islands, even when germanene was present at RT. This behavior indicates the thermal instability of germanene within this temperature range. At 500 °C, all Ge–Ge bonds on the Ag(111) surface are broken, and subsequent cooling to RT leads to germanene formation.

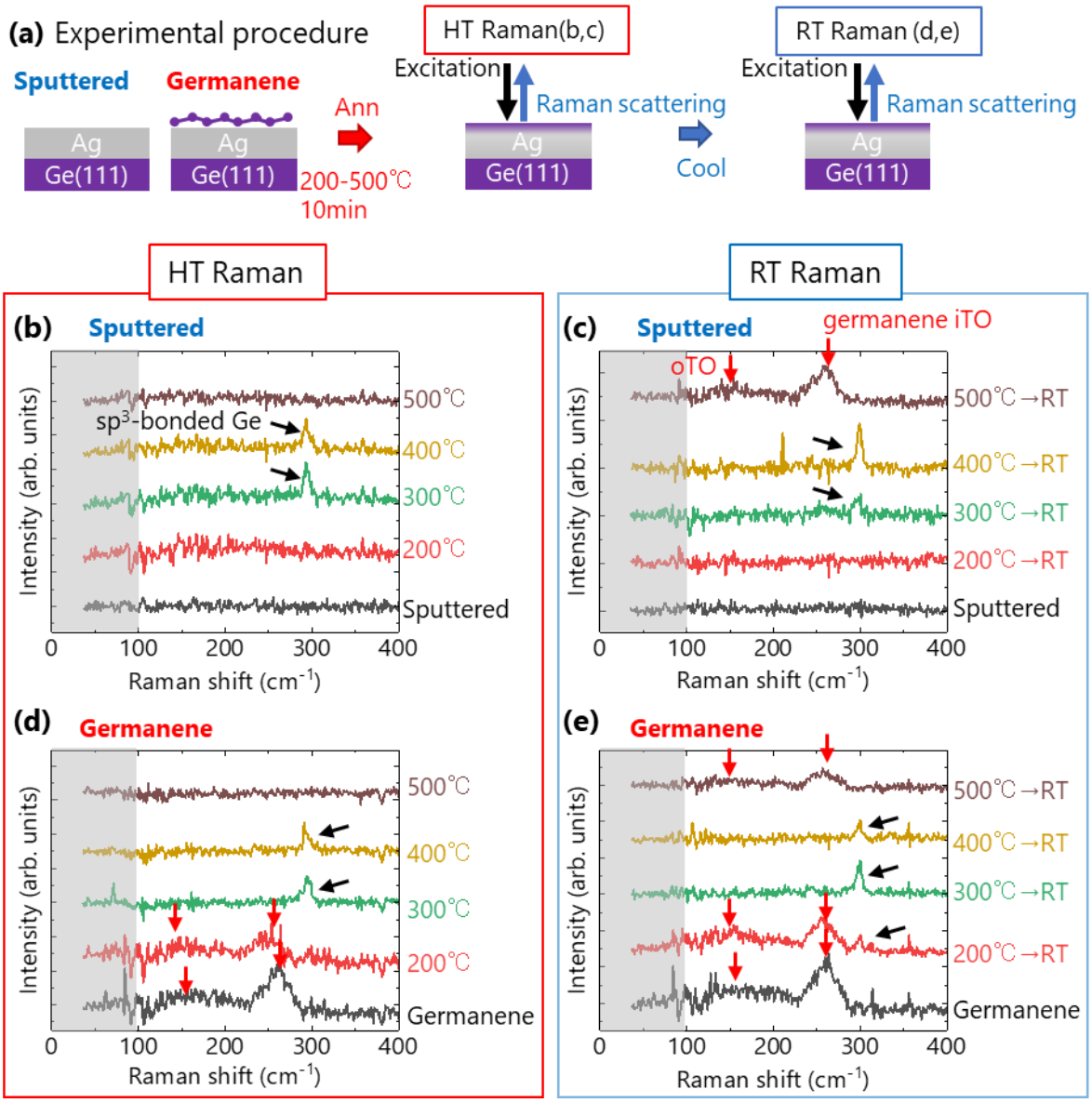

Figure 2. (a) Schematic of experimental procedure for annealing experiments. (b–e) Temperature dependence of Raman spectra of (b, c) sputtered and (d, e) germanene substrates (b, d) at HTs during annealing and (c, e) at RT after annealing. In (b–e), black and red arrows highlight the sp^3-bonded Ge and germanene peaks. The gray background indicates the Raman shift below 100 cm^{-1}, where Rayleigh scattering affects the measurement. Note that the background was subtracted using the spectrum of another sputtered sample.

The role of HT states in the germanene formation process is further examined by XPS (Figures 3, 4). To examine the chemical state and amount of surface Ge, particularly during annealing processes, we performed in situ XPS measurements of the Ge 3d spectra for the pristine, sputtered, and germanene substrates at various HTs during annealing and at RT after cooling (Figure 3a). Comparing these substrates clarifies how the initial Ge distribution on and in Ag affects germanene formation. Representative spectra are shown in Figures 3b–g, with the peak-fitting results in Figures 4a–d. Unless noted, we use the Ge 3d peak area and the Ge 3d/Ag 3d area ratio to estimate the surface Ge amount.

For pristine substrate at HTs (Figure 3b), no Ge 3d peak was observed up to 300 °C during annealing, indicating that Ge atoms have not reached the surface from the Ge(111) through the Ag film. The Ge 3d peak appeared at 350 °C and became more prominent at HTs, and remained at 450 and 500 °C. As the Raman spectra showed no peaks (Figures 2b, d), Ge atoms reside on the surface without forming Ge–Ge bonds at 450 and 500 °C. Cooling to RT increases the Ge 3d signal relative to that at HTs (Figure 3c). This indicates that Ge atoms dissolved in the Ag film at HTs segregate to the Ag(111) surface upon cooling, particularly after annealing at 400–500 °C, leading to an increase in surface Ge.

For sputtered substrates at HTs (Figure 3d), weak Ge 3d peaks were observed before annealing. The Ge amount is estimated to be less than 10% of that in germanene (see Figure 4a), suggesting that the sputtering process removed most of the surface Ge. An increase in the Ge 3d peak intensity was observed at HTs above 200 °C. Compared with the pristine substrate, the surface Ge amount on the sputtered substrate was higher at 200 °C (Figure 3b), indicating that surface Ge mainly originates from the Ge atoms remaining in the Ag(111) thin film rather than from the Ge(111) substrate. During annealing at 300 and 500 °C, the Ge amount remains, suggesting that the near-

surface Ge population was largely maintained under both conditions. After cooling to RT (Figure 3e), the Ge intensity exceeded that at HTs, as was the case for the pristine substrate. Therefore, the pristine and sputtered samples are considered to be in the same state with respect to the Ge 3d intensity trend during annealing at 400–500 °C. Notably, a shoulder emerged around 30.0 eV at 300 °C (Figure 3d) and disappeared at 500 °C. We attribute this component to sp^3-bonded Ge atoms, with Ge $3d_{5/2}$ and $3d_{3/2}$ peaks at 29.39 and 29.94 eV, respectively[34]. The temperature dependence of the shoulder peak in XPS is consistent with the Raman peaks characteristic of 3D Ge islands (Figures 2b–e), supporting its assignment to sp^3-bonded Ge.

On the other hand, for germanene substrates at HTs (Figure 3f), the Ge 3d peak intensity gradually decreased up to 250 °C, suggesting partial dissolution of surface Ge into the Ag film, and then remained nearly constant above 300 °C. Similar to the sputtered substrates, sp^3-bonded Ge was observed in the 250–400 °C range and disappeared at 450–500 °C. At RT after subsequent cooling (Figure 3g), the spectra obtained after 250–400 °C annealing were almost identical to each other, whereas those after 450 and 500 °C annealing deviated markedly from the 250–400 °C spectra. After annealing at 250–400 °C, a peak appeared around 29.3 eV, corresponding to sp^3-bonded Ge. This trend is more pronounced than on the other substrates at those temperatures, suggesting enhanced 3D Ge island formation on this substrate. Since the germanene substrate initially has germanene on the surface, the 3D Ge island formation is likely correlated with a higher initial surface Ge concentration. After cooling to RT following annealing at 450 and 500 °C, the 3D Ge islands disappeared, and germanene re-formed (Figure 3g), as on the other substrates. The peak fitting analysis of Ge 3d at HTs is presented in Figure 4 to further elucidate the mechanism of germanene formation.

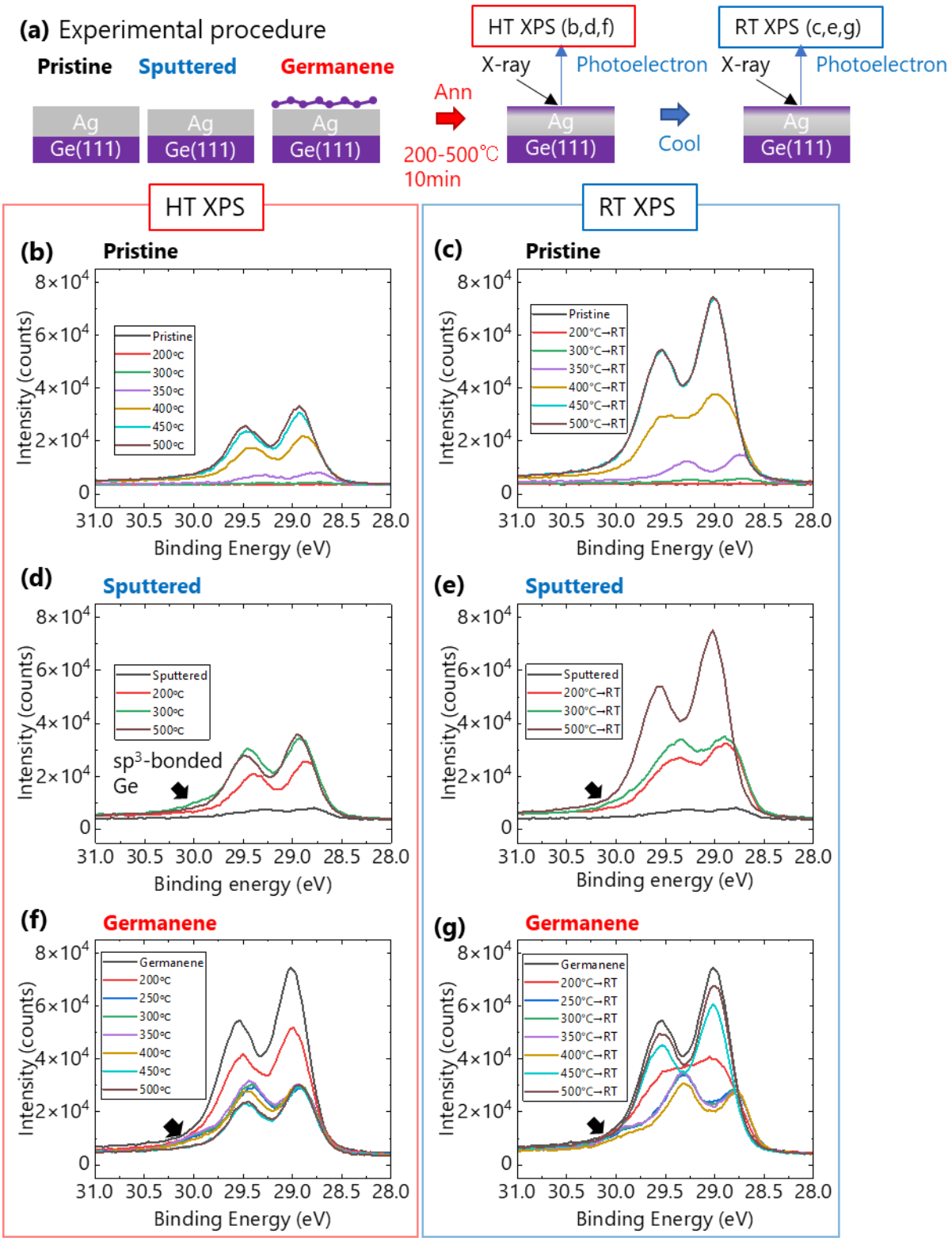
(a) Experimental procedure
Pristine
Sputtered
Germanene
Ag
Ge(111)
Ann
200-500℃
10min
HT XPS (b,d,f)
RT XPS (c,e,g)
X-ray
Photoelectron
Cool
HT XPS
RT XPS
(b) Pristine
(c) Pristine
(d) Sputtered
(e) Sputtered
(f) Germanene
(g) Germanene
Intensity (counts)
Binding Energy (eV)
Binding energy (eV)
sp3-bonded Ge
Pristine
200℃
300℃
350℃
400℃
450℃
500℃
Sputtered
Germanene
250℃
200℃→RT
300℃→RT
350℃→RT
400℃→RT
450℃→RT
500℃→RT

Figure 3. (a) Schematic of experimental procedure for annealing experiments. (b–g) Temperature dependence of XPS Ge 3d spectra of (b, c) pristine, (d, e) sputtered, and (f, g) germanene substrates, (b, d, f) at HTs during annealing and (c, e, g) at RT after annealing. Black arrows highlight the formation of the sp^3-bonded Ge atoms.

To gain quantitative insight into the temperature dependence of the Ge amount on the Ag surface and its chemical states, the peak fitting results are presented in Figures 4a–d. Figures 4a, b, and S4a, b, show the Ge/Ag ratios at HTs and RT, calculated from the Ge and Ag 3d peak area and their photoionization cross sections[35]. Using the photon energy of 700 eV and the binding energies of Ge 3d (~29 eV) and Ag 3d (~368 eV), the inelastic mean free paths were estimated to be 1.58 nm for Ge 3d and 0.674 nm for Ag 3d[36]. In this analysis, the Ge one monolayer (ML) is defined as a Ge(111) bilayer with a thickness of approximately 3.27 Å, corresponding to 1.45×10^{15} atoms cm^{-2}, which gives a Ge/Ag atomic ratio of about 0.422[37]. For spectra that required two components in the fitting, the first component (at the lower binding energy) corresponds to Ge in and on the Ag film. In contrast, the second component (at the higher binding energy) is shown as open symbols in Figures S4a–d and is mainly attributed to sp^3-bonded Ge (Ge $3d_{5/2}$ peak at 29.39 eV).

Figures 4a, b show how the Ge amount varies with temperature across different substrates. For the pristine substrate (Figure 4a), the Ge/Ag atomic ratio starts to increase at 350 °C and reaches a level comparable to that of the other substrates at 400 °C. For the sputtered and germanene substrates, the Ge/Ag ratios at 300–400 °C (Figure 4a) are approximately 0.3, corresponding to 3/4 ML of Ge. This Ge amount exceeds the solubility of Ge in bulk Ag, which is less than 1% at 200 °C and approximately 5% at 500 °C[38], suggesting formation of surface alloys containing Ge. Moreover, the excess Ge remains at the surface after cooling from 300–400 °C (Figures 4b, S4b), consistent with our previous results[29] and earlier studies[5,26].

Upon annealing at 450–500 °C, the surface Ge amounts reached similar levels across the three samples (Figure 4a). As this trend is independent of the initial Ge content, a surface thermodynamic equilibrium within the Ag(111)/Ge(111) segregation system (no external Ge flux) is considered established at 450–500 °C. Consequently, annealing the sample even once to 450 °C or higher causes Ge to inevitably segregate from the Ag to the surface during subsequent cooling to RT. This results in a final Ge surface coverage exceeding 1 ML (corresponding to a Ge/Ag ratio of 0.422) and may correlate with germanene formation, as observed in Raman spectroscopy (Figure 2). These findings suggest that the Ge state at 450–500 °C is a key to form germanene, and elucidating its chemical state is important for understanding the mechanism of germanene formation.

To examine the temperature dependence of the chemical states of Ge, we analyzed the Ge $3d_{5/2}$ peak positions (Figures 4c, d). For the present analysis, we classified Ge into five chemical states (Ge in bulk Ag, Ag_2Ge, site-exchanging Ge atoms, germanene, and sp^3-bonded Ge) based on peak-fitting results as summarized in Figures 5a–e. Here, we focus on the Ag coordination number around Ge. This classification is based on the interpretation that the upward shifts of the Ge 3d peak result from reduced charge transfer from Ag to Ge caused by a lower Ag coordination number around Ge, as detailed below.

We now detail this interpretation by assigning the Ge $3d_{5/2}$ peak positions to specific Ag coordination numbers (Figures 5a–e). The assignments for Figures 5a, b, d, e are based on previously reported binding energies and coordination numbers in the literature[6,26,29,39,40]. The state shown in Figure 5c is newly identified in the present study. The Ge $3d_{5/2}$ peak at 28.7 eV is observed for the pristine substrate after annealing at 300–350 °C (black plot in Figure 4d). We attribute this lowest binding energy to Ge atoms embedded substitutionally in the bulk Ag near the

surface (Figure 5a). In this configuration, each Ge atom is surrounded by twelve Ag atoms[26,39], maximizing the charge transfer from Ag to Ge and lowering the Ge $3d_{5/2}$ binding energy. The peak at approximately 28.8 eV corresponds to the Ag_2Ge surface alloy, where each Ge is coordinated by nine Ag atoms[26] (Figure 5b). This state appears after annealing at 250–350 °C. Consistent with prior work[6,29], the Ge $3d_{5/2}$ peak at ~29.0 eV is assigned to $7\sqrt{7} \times 7\sqrt{7}$ germanene on Ag(111). Because of the superstructure and its buckled lattice, the coordination to Ag can range from 0 to 3 (Figure 5d). At the highest binding energy, around 29.3 eV, the sp^3-bonded Ge (Figure 5e) appears. This state is less coordinated to Ag atoms than the other Ge structures and is associated with 3D Ge islands.

We next discuss the chemical states of Ge during annealing (Figure 4c). We identified an HT state with a distinctive Ge $3d_{5/2}$ component at 28.9 eV. During annealing, the sputtered and germanene substrates reach this state at 250–500 °C, whereas the pristine substrate does so at 400–500 °C. Since 28.9 eV is intermediate between the Ag_2Ge and germanene peak positions, the Ag coordination number around Ge is in the range 3–9 (Figure 5c). Zhang et al. reported that in an in situ STM study, Ge atoms on Ag(111) are highly mobile, repeatedly inserting into and de-inserting from the Ag surface at 107–157 °C[40]. Our observed distinct 28.9 eV state would be considered as an HT state in which insertion and de-insertion of surface Ge are pronounced (Hereafter, this HT state is referred to as "site-exchanging Ge atom"). The in situ XPS results revealed that the aforementioned surface equilibrium state at 450–500 °C represents a single chemical state in the Ag(111)/Ge(111) segregation system, regardless of the initial Ge amount. This convergence at HT enables the highly reproducible formation of $7\sqrt{7} \times 7\sqrt{7}$ germanene on Ag(111) via segregation.

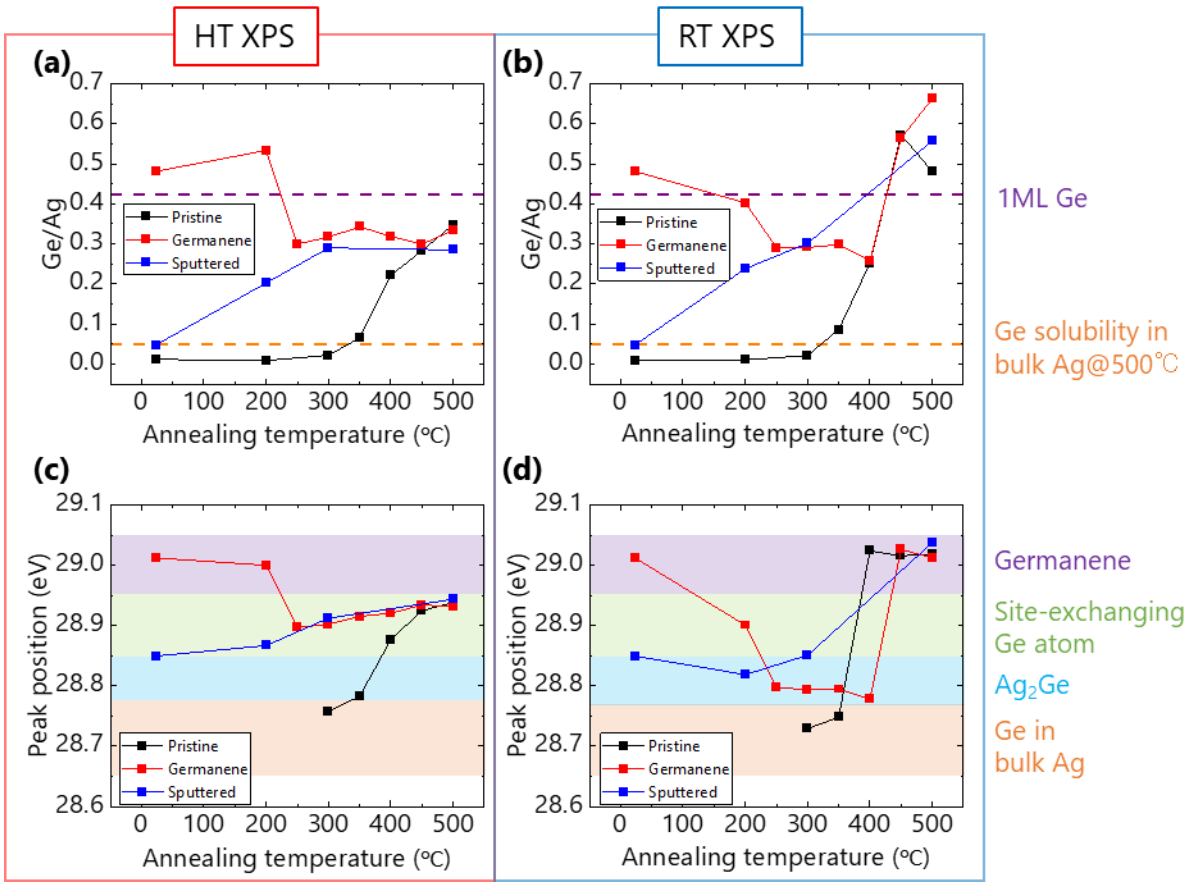

Figure 4. (a, b) Ge amount and (c, d) Ge $3d_{5/2}$ peak position analyses (a, c) at HTs during annealing and (b, d) at RT after annealing. In (c, d), peak assignments for germanene, site-exchanging Ge atoms, Ag_2Ge, and Ge in bulk Ag are indicated in purple, green, light blue, and orange, respectively.

Structural model Side view	Top view	State name	Coordination number	Ge $3d_{5/2}$ (eV)
(a) Surface [111]	[11-2] [-110]	Ge in bulk Ag	12	28.7
(b)		Ag_2Ge	9	28.8
(c)		Site-exchanging Ge atom	3-9	28.9
(d)		Germanene	0-3	29.0
(e)		sp^3-bonded Ge	0-3	29.4

Figure 5. Schematics of Ge chemical states with structural models (side and top views), state name, Ag coordination number around Ge, and binding energy of Ge $3d_{5/2}$ for (a) Ge in bulk Ag, (b) Ag_2Ge, (c) site-exchanging Ge atom, (d) germanene, and (e) sp^3-bonded Ge.

Figure 6 schematically illustrates the effect of annealing temperature on Ge behavior on pristine, sputtered, and germanene substrates (Figures 6a–c), as revealed by Raman spectroscopy and XPS. For the pristine substrate (Figure 6a), the surface condition remains unchanged (no Ge segregation) up to 350 °C and becomes similar to that of the other substrates above 400 °C (Figure 6d). For the sputtered and germanene substrates (Figures 6b, c), the initial states are nearly unchanged from RT up to approximately 200 °C. Between 300–400 °C, Ge atoms dynamically exchange sites near the Ag surface, with a portion of Ge atoms forming 3D Ge islands (Figure 6e). On further heating to 400–500 °C, 3D Ge islands disappear, and site-exchanging Ge atoms stay on the Ag(111) surface (Figure 6d). Upon cooling from 450–500 °C to RT, Ge atoms crystallize into germanene

at RT (Figure 6f). In contrast, annealing at 300–400 °C to RT yields Ag_2Ge, while the residual Ge remains as 3D islands (Figure 6g). Thus, germanene formation via segregation in the Ag(111)/Ge(111) is insensitive to the initial substrate condition, ensuring high reproducibility. These observations underscore the importance of understanding the cooling process from 500 °C (Figures 6d, f), where dynamically site-exchanging Ge atoms form germanene.

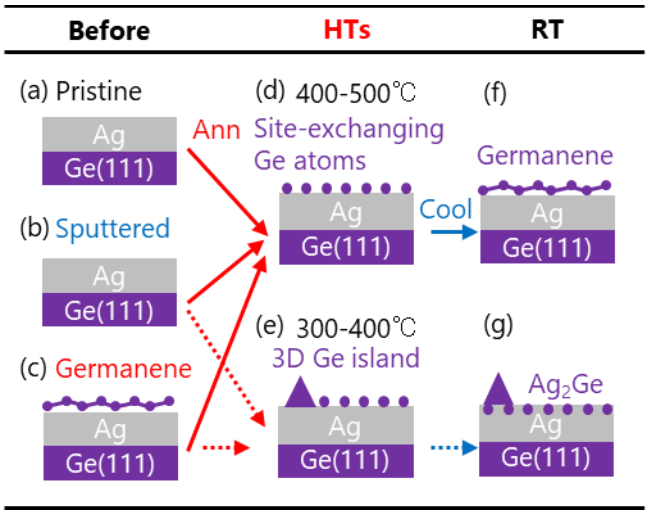

Figure 6. Schematic illustrations of Ge atom behavior depending on temperatures for (a) pristine, (b) sputtered, and (c) germanene substrates. (d, e) The conditions at HTs are illustrated for (d) site-exchanging Ge atoms at 450–500 °C and (e) for those with 3D Ge islands at 300–400 °C. (f, g) After annealing, (f) germanene or (g) Ag_2Ge with 3D Ge islands were observed at RT. The Ag thin film and Ge substrate are illustrated as grey and purple boxes, respectively. Ge atoms are depicted as purple balls. Ge atoms formed a 3D Ge island, shown as purple triangles. The germanene is shown in the ball-and-stick model.

Cooling experiments. Above, it was demonstrated that germanene forms on the Ag(111) surface from 500 °C to RT during cooling. To elucidate how cooling governs germanene formation, we performed in situ Raman spectroscopy and in situ XPS during cooling from 500 °C to RT, pausing at T_{interm} for measurements. A schematic of the experimental procedure for Raman spectroscopy is shown in Figure 7a. Here, the sputtered substrate was used as a representative because the same temperature-dependent behavior was observed on the germanene substrate (Figure S5). Initially, the sample was annealed at 500 °C, followed by the cooling to T_{interm}, at which Raman measurements were conducted. Subsequently, the sample was cooled to RT, and additional Raman measurements were performed at RT.

During the cooling from 500 °C to T_{interm}, Raman spectra showed no germanene at 400 °C, whereas germanene formed upon further cooling to 300–200 °C, as evidenced by characteristic peaks at 153–155 and 244–246 cm^{-1} (Figure 7b). The peak intensities were comparable to those after the cooling to RT (Figure 7c). Moreover, germanene peaks were observed at RT even in samples that had been T_{interm} at 400 °C (Figure 7c). Thus, germanene formation is essentially complete during cooling from 400 to 300 °C (Figure 7d), consistent with our in situ LEED observations (Figure S6).

The cooling experiment also gave information about the stability of germanene at HTs. At 300 °C (a green trace in Figure 7b), the iTO phonon peak appeared at 244 cm^{-1}, 10 cm^{-1} redshift from 254 cm^{-1} at RT. Suzuki et al. reported the iTO phonon peak shifting from 300 to 230 cm^{-1} for −2% (compressive) to +6% (tensile) strain[7]. Therefore, the 255 cm^{-1} peak at RT in this work indicates approximately 3% tensile strain in germanene on Ag(111). On the other hand, the peak position of 244 cm^{-1} at 300 °C implies approximately 4% tensile strain. This 1% increase in strain can be explained by the thermal-expansion mismatch between Ag(111) and germanene.

Specifically, while Ag(111) has a positive thermal expansion coefficient of 1.8×10^{-5} K^{-1} [41], germanene is considered to exhibit a negative one of -2×10^{-6} K^{-1} [42]. As a result, the mismatch in lattice constants between Ag and germanene increases 0.5% with the temperature increase to 300 °C, which is qualitatively consistent with the estimated tensile strain increase in Raman spectra. Moreover, this excessive tensile strain is likely to lead to the structural instability of germanene at 400 °C.

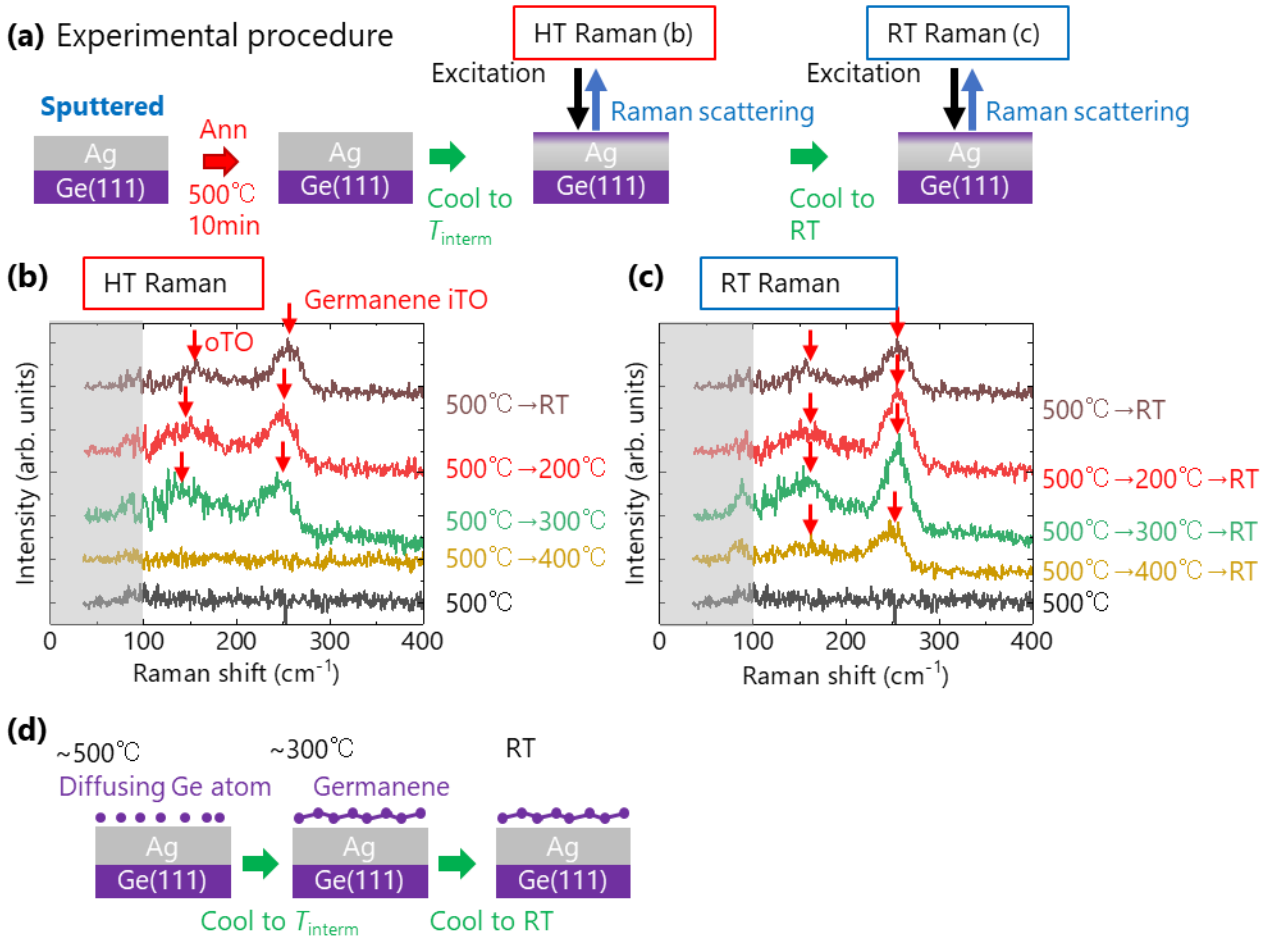

Figure 7. (a) Schematic of experimental procedure for cooling experiments. (b, c) Temperature dependence of Raman spectra after (b) cooling from 500 °C to T_{interm} and (c) cooling from T_{interm}

to RT. Other highlights are the same as in Figure 2. (d) Schematic of germanene formation during cooling from 500 to 300 °C.

Figure 8a presents a schematic of the in situ XPS measurements during cooling. Since HT annealing at 500 °C yields the same state across the three substrates, we use the sputtered substrate as a representative. After annealing at 500 °C for 10 minutes, the sample was cooled to the designated T_{interm} of 200, 250, and 300 °C, and XPS measurements were performed at the T_{interm}. The sample was then further cooled to RT, followed by XPS measurements at RT. Figures 8b, c show the Ge 3d XPS spectra obtained at the T_{interm} and RT, respectively. After the cooling to T_{interm} (Figure 8b), an increase in the Ge 3d peak intensity was observed, indicating the segregation of Ge atoms. Following the cooling to RT, the Ge 3d peak intensity remained almost unchanged compared to the T_{interm} at 200–300 °C (Figures 8b, c), indicating that 300 °C essentially completed Ge segregation. The green plots in Figures 8d, e show the results of the peak-fitting analysis for the cooling experiments. Note that the red plots indicate the results of annealing experiments on the germanene substrate for comparison. In Figure 8d, the Ge amount increased during cooling from 500 to 300 °C (green plots), reaching Ge/Ag ~0.5, corresponding to more than 1 ML of Ge. Upon decreasing the T_{interm} from 300 °C to RT, a slight increase in Ge/Ag was observed. As shown in Figure 8e, the cooling to RT also results in only a slight increase in the Ge amount from 300 °C to RT. Thus, Ge/Ag reaches ~0.5 at 300 °C by cooling and changes only slightly on further cooling to RT. In contrast, when germanene samples were annealed (red plots in Figure 8d) between 200 and 250 °C, the Ge/Ag ratio decreased markedly, reaching ~0.3 at 300 °C.

Despite both cases reaching 300 °C, the heating and cooling experiments revealed that samples cooled from 500 to 300 °C yielded a higher Ge content (Figure 8) and formed germanene (Figure 7). In contrast, those heated from RT to 300 °C showed lower Ge amounts (Figures 3, 4) and

formed 3D Ge islands (Figure 2). The differing surface phases at 300 °C indicate strong path dependence, suggesting that surface structure formation is governed by the kinetics of Ge segregation rather than thermodynamic equilibrium. The kinetics of Ge segregation will be analyzed in the Discussion section.

Figures 8f, g present the results of the chemical state analysis by peak position. After the cooling to T_{interm}, the Ge $3d_{5/2}$ peaks shifted to 29.00–29.05 eV, as shown by the green plots in Figure 8f. This peak position indicates that Ge formed germanene at 300 °C, consistent with the results shown in Figure 7. As shown in the peak positions in Figure 8g, these samples retained the germanene structure after cooling to RT. In contrast, heating the germanene sample from RT to 300 °C (red plots in Figure 8f) led to a surface state of site-exchanging Ge atoms, which transformed into Ag_2Ge at RT (Figure 8g). Hence, the chemical state of Ge at 300 °C depends on whether the temperature is approached by cooling or heating.

The contrasting behavior between heating and cooling was also interpreted as a temperature-hysteresis characteristic of germanene formation and deformation. Germanene disappeared during annealing at 200–250 °C (Figures 2d, e and 4c, d) and reformed during cooling from 500 °C to 300–400 °C (Figures 7b, c and 8f, g), resulting in a temperature hysteresis of approximately 50–100 °C. This behavior contrasts with graphene segregation on Ni, where the equilibrium transition width is only about 15 °C [43]. Furthermore, in typical hysteresis associated with equilibrium transitions, the transition temperature during cooling is lower than that during heating[43]. In this study, however, the phase transition occurred at a higher temperature during cooling (between 300 and 400 °C) than during heating (between 200 and 250 °C). This reversed hysteresis may reflect the influence of kinetic constraints, such as the slow diffusion of Ge through the Ag thin film.

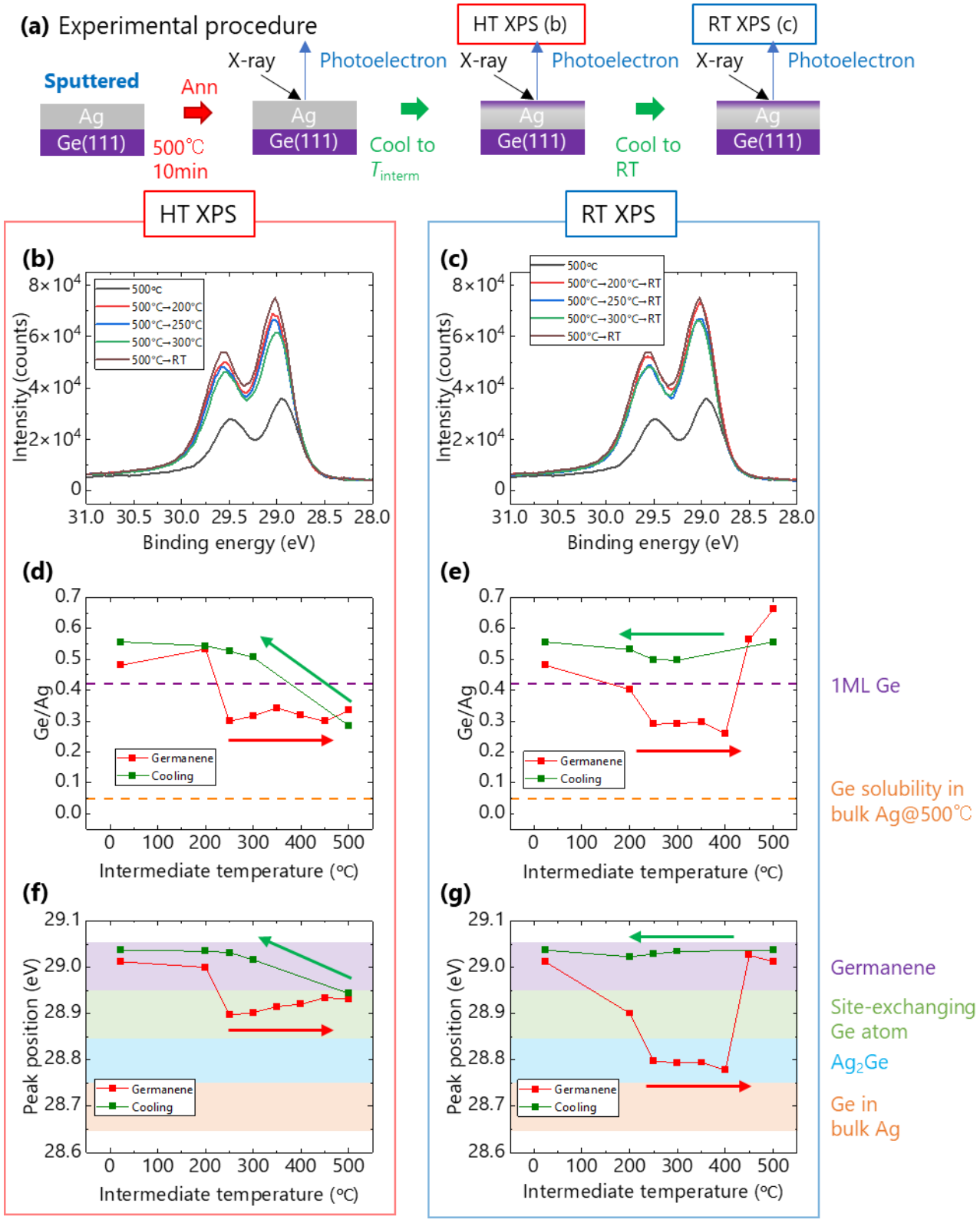
(a) Experimental procedure
Sputtered
Ag
Ge(111)
Ann
500℃
10min
X-ray
Photoelectron
Cool to
T_{interm}
HT XPS (b)
Cool to
RT
RT XPS (c)
HT XPS
RT XPS
(b)
(c)
Intensity (counts)
Binding energy (eV)
500℃
500℃→200℃
500℃→250℃
500℃→300℃
500℃→RT
(d)
(e)
Ge/Ag
Germanene
Cooling
Intermediate temperature (℃)
1ML Ge
Ge solubility in
bulk Ag@500℃
(f)
(g)
Peak position (eV)
Germanene
Site-exchanging
Ge atom
Ag_2Ge
Ge in
bulk Ag

Figure 8. (a) Schematic of experimental procedure for cooling experiments. (b, c) Temperature dependence of XPS Ge 3d spectra after (b) cooling from 500 °C to T_{interm} and (c) cooling from T_{interm} to RT. (d, e) Ge/Ag and Ge 3d peak position analyses. In (d, e), data for the sputtered substrate during cooling experiments and for germanene substrates during annealing experiments are shown in green and red plots, respectively. Only the primary component (filled red) is depicted for simplicity. Other highlights are the same as in Figures 3, 4.

DISCUSSION

Temperature-dependent diffusion analysis. To elucidate the mechanism of germanene formation, we focus on the diffusion of Ge atoms through the Ag thin film. As discussed in Figure 4c, Ge chemical states at HTs (300–500 °C) are similar for the sputtered and germanene substrates. In contrast, the pristine substrate shows a different state up to 400 °C, even after 10 minutes of annealing. This difference indicates that the Ge diffusion through the 150-nm-thick Ag film is a slower, minute-scale process compared to the germanene formation of μm-size in a second-scale[10]. Therefore, we suggest that the kinetic bottleneck in germanene formation is the Ge supply from the Ag thin film to the surface.

To better understand the temperature-dependent behavior of Ge, we calculated the one-dimensional diffusion of Ge atoms in Ag. It follows the relation $D = D_0 \exp(-E_a/k_B T)$, where D is the interdiffusion coefficient of Ge in Ag, D_0 is the pre-exponential factor, E_a is the activation energy for Ge diffusion in bulk Ag, k_B is the Boltzmann constant, and T is the temperature. According to the literature, D_0 and E_a have been reported as 8.4×10^{-6} m^2/s and 1.583 eV/atom, respectively[44]. Table 1 presents the temperature dependence of D and Ge diffusion length $\lambda = \sqrt{(Dt)}$

in Ag, where t is time. Here, t was taken as 600 seconds, corresponding to the annealing duration in our experiments (10 minutes). Based on λ, we discuss the temperature-dependent experimental observations.

Table 1. Temperature dependence of diffusion constant and diffusion length.

	200°C	300°C	400°C	500°C
D (m^2/sec)	$1.16 \pm 0.06 \times 10^{-22}$	$1.01 \pm 0.05 \times 10^{-19}$	$1.18 \pm 0.06 \times 10^{-17}$	$4.0 \pm 0.2 \times 10^{-16}$
$\lambda=\sqrt{Dt}$ (nm)	0.264 ± 0.007	7.8 ± 0.2	84 ± 2	490 ± 10

Ge atom dynamics and growth model of germanene. We first consider the dynamics of Ge atoms during cooling from 500 to 300 °C, during which germanene forms. At 500 °C, the Ag thin film is saturated with Ge, and mobile Ge atoms are present on the Ag surface (bottom of Figure 9). This saturated state at 500 °C serves as the starting point for discussing the subsequent cooling process. During cooling from 500 to 400 °C, the solubility of Ge in Ag decreases, and Ge atoms become less stable within the Ag lattice, leading to a net Ge flux in the Ag film directed toward both the surface and the Ge(111) substrate. In this temperature range, however, λ is still longer than the Ag film thickness, allowing Ge atoms to continue diffusing toward the thermodynamically favored Ge(111) substrate rather than the surface.

By contrast, upon further cooling to 300 °C (thick green arrow in Figure 9), the solubility of Ge in Ag further decreases, and λ becomes shorter than the Ag film thickness. Under these conditions, Ge atoms can no longer diffuse throughout the entire Ag layer to reach the Ge(111) substrate, as they do at 500 °C (purple arrow); instead, they segregate at the surface, increasing the surface Ge concentration. For the Ag(111) of 150 nm used in our experiments, the approximately 2% decrease

in Ge solubility from 400 to 300 °C would supply enough Ge to form up to six germanene layers. However, the XPS results show that only one germanene layer actually forms, and subsequent multilayer formation was suppressed. This observation suggests the presence of a self-limiting mechanism during germanene growth.

Such results indicate that, once a monolayer of germanene forms on Ag(111), it becomes kinetically stabilized against further segregation. Such stabilization likely occurs when the Ag film is saturated with Ge and the surface Ge concentration is high, which energetically favors the formation of a two-dimensional germanene layer over the growth of 3D Ge islands. Indeed, density functional theory calculations have shown that the formation of the germanene lattice is more favorable with increasing Ge coverage on Ag(111)[45], implying that a high surface concentration of Ge promotes the metastable stabilization of monolayer germanene. When the germanene phase is stabilized and covers the entire surface, it is less likely for Ge in Ag to penetrate through the germanene and segregate more, thereby suppressing multilayer formation. This self-limiting behavior is insensitive to the specific annealing profile or the T_{interm} during cooling, suggesting that it is an intrinsic feature of germanene formation via segregation. Note that because λ decreases exponentially with decreasing temperature, it becomes shorter than the film thickness around 300–400 °C for typical Ag(111) film thicknesses (50–300 nm) used in experiments. Thus, the germanene formation temperature is almost independent of the Ag(111) film thickness.

In addition to the cooling process, the behavior of Ge during annealing can also be rationalized within the same framework of temperature-dependent solubility and diffusion length (see also Supplementary Discussion for details). As the temperature of germanene (thick red arrow from top-right in Figure 9) increases, the solubility of Ge in Ag rises, and Ge atoms become thermodynamically less stable on the Ag surface. This drives a net flux of Ge atoms from the

Ag(111) surface into the Ag thin film. At the beginning of annealing, when the temperature is still low, such as 300 °C, λ is shorter than the Ag film thickness, and Ge atoms remain localized near their initial states. As the temperature increases to 500 °C, however, λ exceeds the film thickness, enabling Ge atoms to freely diffuse throughout the entire Ag layer. Consequently, the Ag thin film becomes saturated with Ge at 500 °C, as illustrated at the bottom of Figure 9.

Thus, the temperature-dependent solubility of Ge in the Ag thin film drives the Ge diffusion, while the direction of net Ge flux reverses for heating and cooling. During heating, the increase in Ge solubility in Ag drives Ge atoms from both the surface and the Ge(111) substrate into the Ag thin film, leading to the saturation of the Ag layer with Ge at high temperatures. During cooling, Ge atoms diffuse out of the Ag film due to the limited solubility, leading to a surface Ge concentration exceeding the equilibrium value and favoring the formation of metastable germanene. A sufficient λ is required to supply Ge from the Ag thin film. Consequently, cooling from 500 °C yields germanene, whereas cooling from 300 °C provides insufficient Ge supply and yields Ag_2Ge (see also Supplementary Discussion for details). Therefore, germanene growth via segregation is governed by the Ge-Ag solubility and diffusion length, which together determine the conditions for reproducible, monolayer-selective formation.

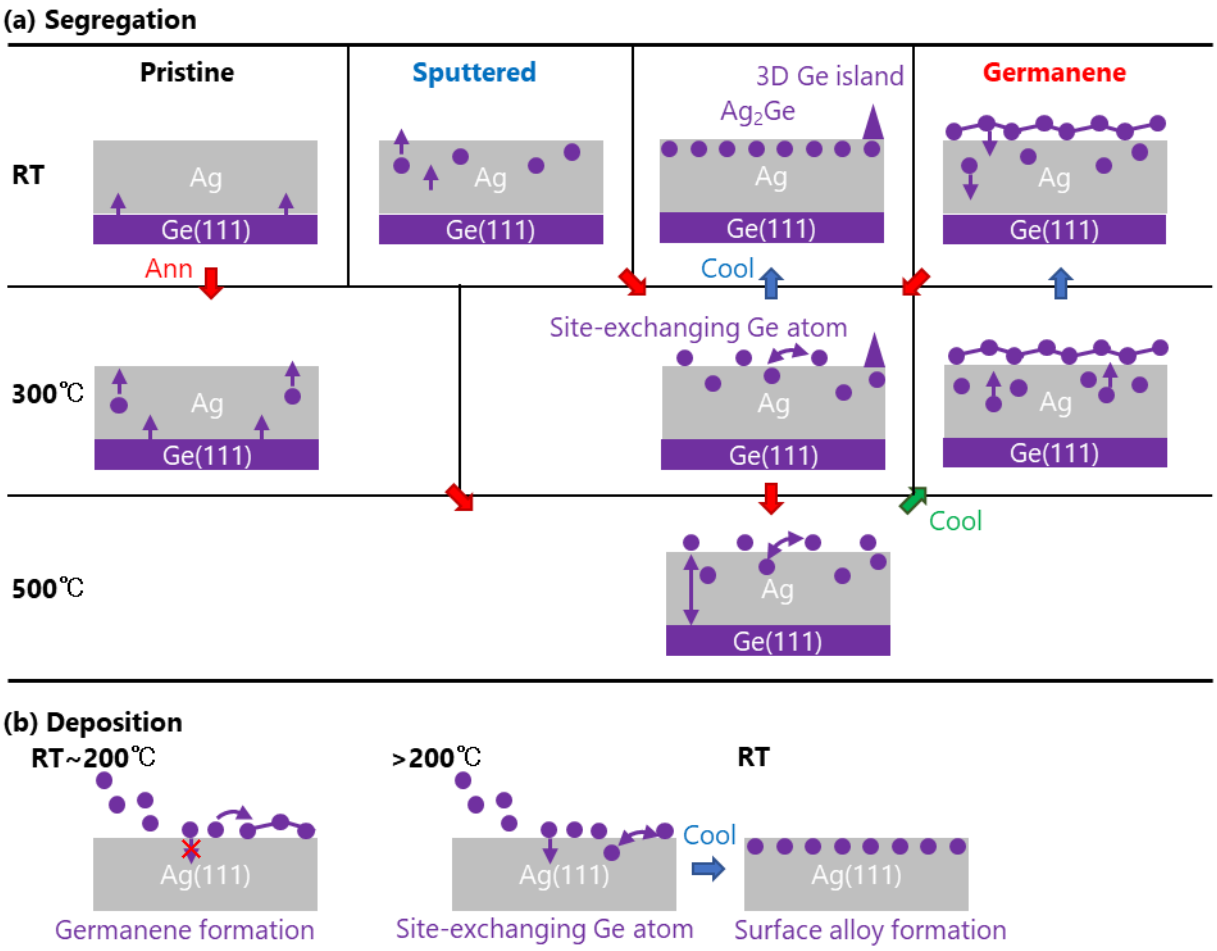

Figure 9. (a) Systematic diagram of surface states achievable by annealing-cooling processes in the Ge segregation system on Ag(111)/Ge(111). The diagram illustrates the states of Ge atoms in and on the Ag thin film at RT, 300, and 500 °C, as well as the transitions between these states. Grey Ag thin films are deposited on purple Ge(111) substrates. Ge atoms forming 3D Ge islands, germanene, site-exchanging Ge atoms, and dissolved Ge in Ag are depicted as purple triangles, ball-and-stick models, balls on Ag, and balls in Ag, respectively. Thin purple arrows indicate the behavior of Ge atoms at each temperature, representing site exchange on the surface above 300 °C and overall equilibrium in the system at 500 °C. Thick arrows in red, blue, and green indicate heating, cooling from 300 °C, and cooling from 500 °C, respectively. Thin arrows of the same

colors represent the corresponding diffusion direction and relative diffusion length of Ge atoms. (b) Schematic illustration of germanene formation via deposition method.

Comparison with other systems. Finally, we would like to compare our growth model with other systems. We found that the Ge-enriched surface observed during cooling can be attributed to the long λ at HTs. This is likely due to the high eutectic temperature of the Ge–Ag system (~600 °C), which keeps the system solid and allows extensive diffusion before melting would otherwise occur. By the same reasoning, Ge–Cu, Sn–Au, Sn–Cu, and Pb-Pd systems are promising candidates for segregation growth of monolayer germanene, stanene, and plumbene, because these systems have high eutectic temperatures and monolayer formation has been reported on the corresponding metal substrates using deposition methods[16,46–48].

Next, we discuss the differences between the Ge deposition and segregation. During Ge deposition on Ag(111) single-crystal substrates (Figure 9b), the typical growth temperature for germanene formation is capped at approximately 200 °C because Ge diffuses rapidly into the bulk Ag at higher temperatures, depleting the surface Ge concentration. The deposition rate and temperature must be precisely controlled to grow the metastable germanene while avoiding reaching thermal equilibrium. In Ge deposition on an Ag(111) single-crystal substrate, the Ag beneath the germanene remains unsaturated with Ge at the growth temperature, often resulting in insufficient surface Ge supply, consistent with the reported Ge vacancies substituted by Ag[9].

In contrast, the present study demonstrated that germanene can be stably maintained by cooling from 500 to 300 °C via the Ge segregation on Ag(111). This enables post-growth chemical treatments and device-oriented processing at temperatures of up to 300 °C, which is higher than the temperature achievable with the Ge deposition method. For example, surface functionalization

to prevent the oxidation of germanene can be carried out under thermally activated conditions. By analogy with Au intercalation at the graphene and Ni interface[49], intercalation of foreign atoms at the germanene-Ag interface near 300 °C may also facilitate delamination of germanene from the Ag(111) surface. Thus, segregation-based growth not only improves reproducibility and monolayer selectivity but also opens practical routes to advancing germanene chemistry and device integration.

CONCLUSIONS

In summary, we investigated the growth process of germanene using the Ge-segregation method, employing in situ Raman spectroscopy and XPS. We observed that 3D Ge islands form at 300 °C and disappear at 500 °C. We revealed that site-exchanging Ge atoms appear at 500 °C and they are important for germanene formation upon subsequent cooling. The temperature-dependent Ge diffusion length and solubility in Ag were identified as key parameters for germanene formation, thereby ensuring experimental reproducibility. Particularly, the intrinsic stability of monolayer germanene, achieved via the Ge segregation method, is confirmed. This kinetic pathway, distinct from the deposition method, enables the formation of uniform, thermally stable germanene without requiring precise process control. We expect our findings to apply to the growth of 2D materials other than germanene via the segregation method. The insights obtained here not only clarify the growth mechanism but also provide a platform for surface chemical treatments and potential delamination strategies, expanding the applicability of germanene in device integration and HT surface chemistry.

ASSOCIATED CONTENT

Supporting Information. The Supporting Information is available free of charge at. File contents: additional experimental data, including XPS and Raman spectra, optical micrograph, and LEED data, together with additional discussion about the growth mechanism (PDF)

AUTHOR INFORMATION

Corresponding Author

Tomo-o Terasawa – Advanced Science Research Center, Japan Atomic Energy Agency, 2-4, Shirakata, Tokai, Ibaraki, 319-1195, Japan, Institute of Industrial Science, The University of Tokyo, 4-6-1, Komaba, Meguro, Tokyo, 153-0064, Japan; ORCID; Email: terasawa.tomoo@jaea.go.jp.

Authors

Daiki Katsube – Japan Fine Ceramics Center, 2-4-1, Mutsuno, Atsuta, Nagoya, 456-8587, Japan; ORCID 0000-0001-8879-0163

Masahiro Yano – Advanced Science Research Center, Japan Atomic Energy Agency, 2-4, Shirakata, Tokai, Ibaraki, 319-1195, Japan; ORCID

Takahiro Ozawa – Institute of Industrial Science, The University of Tokyo, 4-6-1, Komaba, Meguro, Tokyo, 153-0064, Japan; ORCID 0000-0001-9930-7018

Yasutaka Tsuda – Materials Sciences Research Center, Japan Atomic Energy Agency, 1-1-1 Kouto, Sayo, Hyogo, 679-5148, Japan; ORCID 0000-0003-4992-6237

Akitaka Yoshigoe – Materials Sciences Research Center, Japan Atomic Energy Agency, 1-1-1 Kouto, Sayo, Hyogo, 679-5148, Japan; ORCID 0000-0002-6332-7743

Hidehito Asaoka – Advanced Science Research Center, Japan Atomic Energy Agency, 2-4, Shirakata, Tokai, Ibaraki, 319-1195, Japan; ORCID

Seiya Suzuki – Advanced Science Research Center, Japan Atomic Energy Agency, 2-4, Shirakata, Tokai, Ibaraki, 319-1195, Japan; ORCID 0000-0003-2445-7462

Author Contributions

The manuscript was written with contributions from all authors. All authors have approved the final version of the manuscript.

Notes

The authors declare no competing financial interest.

ACKNOWLEDGMENT

This study was supported in part by Japan Science and Technology Agency (JST), Precursory Research for Embryonic Science and Technology (PRESTO) Grant Number JPMJPR21B7; Japan Society for the Promotion of Science (JSPS) KAKENHI Grant Number 26420289, 19H05789, 20K05338, 23H01811, 23K26504, 23K26540, and 24K01407; MEXT Leading Initiative for Excellent Young Researchers Grant Number JPMXS0320210036; the JAEA Funds for the President's discretion, Exploratory Researches (Houga fund), and the Reimei Research Promotion project. The synchrotron radiation experiments were performed at the BL23SU surface chemistry experimental station of SPring-8 with the approval of the Japan Synchrotron Radiation Research

Institute (JASRI) (Proposal No. 2022A3801, No. 2022B3801, No. 2023A3801, No. 2023B3801, No. 2024A3801). T. T. acknowledges the Kumagai Science and Technology Promotion Foundation for its grant support.

REFERENCES

(1) Liu, C. C.; Feng, W.; Yao, Y. Quantum Spin Hall Effect in Silicene and Two-Dimensional Germanium. *Phys Rev Lett* 2011, *107* (7), 1–4. https://doi.org/10.1103/PhysRevLett.107.076802.

(2) Acun, A.; Zhang, L.; Bampoulis, P.; Farmanbar, M.; Van Houselt, A.; Rudenko, A. N.; Lingenfelder, M.; Brocks, G.; Poelsema, B.; Katsnelson, M. I.; Zandvliet, H. J. W. Germanene: The Germanium Analogue of Graphene. *Journal of Physics Condensed Matter* 2015, *27* (44). https://doi.org/10.1088/0953-8984/27/44/443002.

(3) Weber, B.; Fuhrer, M. S.; Sheng, X.; Yang, S. A.; Thomale, R.; Shamim, S.; Molenkamp, L. W.; Cobden, D.; Pesin, D.; Zandvliet, H. J. W.; Bampoulis, P.; Claessen, R.; Menges, F. R.; Gooth, J.; Felser, C.; Shekhar, C.; Tadich, A.; Zhao, M.; Edmonds, M. T.; Jia, J.; Bieniek, M.; Väyrynen, J. I.; Culcer, D.; Muralidharan, B.; Nadeem, M. 2024 Roadmap on 2D Topological Insulators. *Journal of Physics: Materials* 2024, *7* (2), 022501. https://doi.org/10.1088/2515-7639/ad2083.

(4) Zhao, A.; Wang, B. Two-Dimensional Graphene-like Xenes as Potential Topological Materials. *APL Mater* 2020, *8* (3), 0–12. https://doi.org/10.1063/1.5135984.

(5) Lin, C.-H.; Huang, A.; Pai, W. W.; Chen, W.-C.; Chen, T.-Y.; Chang, T.-R.; Yukawa, R.; Cheng, C.-M.; Mou, C.-Y.; Matsuda, I.; Chiang, T.-C.; Jeng, H.-T.; Tang, S.-J. Single-Layer Dual Germanene Phases on Ag(111). *Phys Rev Mater* 2018, *2* (2), 024003. https://doi.org/10.1103/PhysRevMaterials.2.024003.

(6) Yuhara, J.; Shimazu, H.; Ito, K.; Ohta, A.; Araidai, M.; Kurosawa, M.; Nakatake, M.; Le Lay, G. Germanene Epitaxial Growth by Segregation through Ag(111) Thin Films on Ge(111). *ACS Nano* 2018, *12* (11), 11632–11637. https://doi.org/10.1021/acsnano.8b07006.

(7) Suzuki, S.; Iwasaki, T.; De Silva, K. K. H.; Suehara, S.; Watanabe, K.; Taniguchi, T.; Moriyama, S.; Yoshimura, M.; Aizawa, T.; Nakayama, T. Direct Growth of Germanene at Interfaces between Van Der Waals Materials and Ag(111). *Adv Funct Mater* 2021, *31* (5), 1–9. https://doi.org/10.1002/adfm.202007038.

(8) Kesper, L.; Hochhaus, J. A.; Schmitz, M.; Schulte, M. G. H.; Berges, U.; Westphal, C. Tracing the Structural Evolution of Quasi-Freestanding Germanene on Ag(111). *Sci Rep* 2022, *12* (1), 7559. https://doi.org/10.1038/s41598-022-10943-0.

(9) Zhang, K.; Hanf, M. C.; Bernard, R.; Borensztein, Y.; Cruguel, H.; Resta, A.; Garreau, Y.; Vlad, A.; Coati, A.; Sciacca, D.; Grandidier, B.; Derivaz, M.; Pirri, C.; Sonnet, P.; Stephan, R.; Prévot, G. The Ground State of Epitaxial Germanene on Ag(111). *ACS Nano* 2023, *17* (16), 15687–15695. https://doi.org/10.1021/acsnano.3c02821.

(10) Hibino, H.; Ohta, A.; Kageshima, H.; Yuhara, J. Low-Energy Electron Microscopy Investigation of Germanene Segregation on Ag(111) Thin Films. *Jpn J Appl Phys* 2025, *64* (5), 050906. https://doi.org/10.35848/1347-4065/add639.

(11) Mizuno, S.; Ohta, A.; Suzuki, T.; Kageshima, H.; Yuhara, J.; Hibino, H. Correlation between Structures and Vibration Properties of Germanene Grown by Ge Segregation. *Applied Physics Express* 2021, *14* (12), 125501. https://doi.org/10.35848/1882-0786/ac3185.

(12) Yuhara, J.; Maeda, S.; Katsube, D.; Suzuki, S.; Terasawa, T.; Takakura, S.; Nakatake, M.; Le Lay, G. Phase Transition of Germanene Prepared by Atomic Segregation Epitaxy at Ag(111) Thin Films on Ge(111). *2d Mater* 2025, *12* (4), 045023. https://doi.org/10.1088/2053-1583/ae1490.

(13) Dávila, M. E.; Xian, L.; Cahangirov, S.; Rubio, A.; Le Lay, G. Germanene: A Novel Two-Dimensional Germanium Allotrope Akin to Graphene and Silicene. *New J Phys* 2014, *16* (9), 095002. https://doi.org/10.1088/1367-2630/16/9/095002.

(14) Dávila, M. E.; Le Lay, G. Few Layer Epitaxial Germanene: A Novel Two-Dimensional Dirac Material. *Sci Rep* 2016, *6* (August 2015), 1–9. https://doi.org/10.1038/srep20714.

(15) Zhuang, J.; Gao, N.; Li, Z.; Xu, X.; Wang, J.; Zhao, J.; Dou, S. X.; Du, Y. Cooperative Electron-Phonon Coupling and Buckled Structure in Germanene on Au(111). *ACS Nano* 2017, *11* (4), 3553–3559. https://doi.org/10.1021/acsnano.7b00687.

(16) Qin, Z.; Pan, J.; Lu, S.; Shao, Y.; Wang, Y.; Du, S.; Gao, H. J.; Cao, G. Direct Evidence of Dirac Signature in Bilayer Germanene Islands on Cu(111). *Advanced Materials* 2017, *29* (13), 1–5. https://doi.org/10.1002/adma.201606046.

(17) Derivaz, M.; Dentel, D.; Stephan, R.; Hanf, M.-C.; Mehdaoui, A.; Sonnet, P.; Pirri, C. Continuous Germanene Layer on Al(111). *Nano Lett* 2015, *15* (4), 2510–2516. https://doi.org/10.1021/acs.nanolett.5b00085.

(18) Fukaya, Y.; Matsuda, I.; Feng, B.; Mochizuki, I.; Hyodo, T.; Shamoto, S. Asymmetric Structure of Germanene on an Al(111) Surface Studied by Total-Reflection High-Energy Positron Diffraction. *2d Mater* 2016, *3* (3), 035019. https://doi.org/10.1088/2053-1583/3/3/035019.

(19) Endo, S.; Kubo, O.; Nakashima, N.; Iwaguma, S.; Yamamoto, R.; Kamakura, Y.; Tabata, H.; Katayama, M. √3x√3 Germanene on Al (111) Grown at Nearly Room Temperature. *Applied Physics Express* 2018, *11* (111), 019201.

(20) Yuhara, J.; Muto, H.; Araidai, M.; Kobayashi, M.; Ohta, A.; Miyazaki, S.; Takakura, S. I.; Nakatake, M.; Lay, G. Le. Single Germanene Phase Formed by Segregation through

Al(111) Thin Films on Ge(111). *2d Mater* 2021, *8* (4). https://doi.org/10.1088/2053-1583/ac2bef.

(21) Li, L.; Lu, S. Z.; Pan, J.; Qin, Z.; Wang, Y. Q.; Wang, Y.; Cao, G. Y.; Du, S.; Gao, H. J. Buckled Germanene Formation on Pt(111). *Advanced Materials* 2014, *26* (28), 4820–4824. https://doi.org/10.1002/adma.201400909.

(22) Yuhara, J.; Matsuba, D.; Ono, M.; Ohta, A.; Miyazaki, S.; Araidai, M.; Takakura, S.; Nakatake, M.; Le Lay, G. Formation of Germanene with Free-Standing Lattice Constant. *Surf Sci* 2023, *738* (March), 122382. https://doi.org/10.1016/j.susc.2023.122382.

(23) Zhang, L.; Bampoulis, P.; Rudenko, A. N.; Yao, Q.; Van Houselt, A.; Poelsema, B.; Katsnelson, M. I.; Zandvliet, H. J. W. Structural and Electronic Properties of Germanene on MoS2. *Phys Rev Lett* 2016, *116* (25), 1–6. https://doi.org/10.1103/PhysRevLett.116.256804.

(24) Persichetti, L.; Jardali, F.; Vach, H.; Sgarlata, A.; Berbezier, I.; Crescenzi, M. De; Balzarotti, A. Van Der Waals Heteroepitaxy of Germanene Islands on Graphite. *Journal of Physical Chemistry Letters* 2016, *7* (16), 3246–3251. https://doi.org/10.1021/acs.jpclett.6b01284.

(25) Bampoulis, P.; Castenmiller, C.; Klaassen, D. J.; Van Mil, J.; Liu, Y.; Liu, C. C.; Yao, Y.; Ezawa, M.; Rudenko, A. N.; Zandvliet, H. J. W. Quantum Spin Hall States and Topological Phase Transition in Germanene. *Phys Rev Lett* 2023, *130* (19), 196401. https://doi.org/10.1103/PhysRevLett.130.196401.

(26) Oughaddou, H.; Sawaya, S.; Goniakowski, J.; Aufray, B.; Le Lay, G.; Gay, J. M.; Tréglia, G.; Bibérian, J. P.; Barrett, N.; Guillot, C.; Mayne, A.; Dujardin, G. Ge/Ag(111) Semiconductor-on-Metal Growth: Formation of an <math Display="inline"> <mrow> <msub> <mrow> <mi Mathvariant="normal">Ag</Mi> </Mrow> <mrow> <mn>2</Mn> </Mrow> </Msub> </Mrow> <mi Mathvariant="normal">Ge</Mi> </Math> Surface Alloy. *Phys Rev B* 2000, *62* (24), 16653–16656. https://doi.org/10.1103/PhysRevB.62.16653.

(27) Liu, Y.; Zhuang, J.; Liu, C.; Wang, J.; Xu, X.; Li, Z.; Zhong, J.; Du, Y. Role of Atomic Interaction in Electronic Hybridization in Two-Dimensional Ag2Ge Nanosheets. *Journal of Physical Chemistry C* 2017, *121* (31), 16754–16760. https://doi.org/10.1021/acs.jpcc.7b02017.

(28) Wang, W.; Sohail, H. M.; Osiecki, J. R.; Uhrberg, R. I. G. Broken Symmetry Induced Band Splitting in the <math> <msub> <mi>Ag</Mi> <mn>2</Mn> </Msub> <mi>Ge</Mi> </Math> Surface Alloy on Ag(111). *Phys Rev B* 2014, *89* (12), 125410. https://doi.org/10.1103/PhysRevB.89.125410.

(29) Suzuki, S.; Katsube, D.; Yano, M.; Tsuda, Y.; Terasawa, T.; Ozawa, T.; Fukutani, K.; Kim, Y.; Asaoka, H.; Yuhara, J.; Yoshigoe, A. Germanene Reformation from Oxidized Germanene on Ag(111)/Ge(111) by Vacuum Annealing. *Small Methods* 2025, *9* (3), 1–9. https://doi.org/10.1002/smtd.202400863.

(30) Chen, T.-Y.; Chen, C.; Mikolas, D.; Chiniwar, S.; Huang, A.; Lin, C.; Cheng, C.; Komori, F.; Matsuda, I.; Mou, C.; Jeng, H.; Pai, W. W.; Tang, S.-J. Striped-Phase Germanene Confirmed by Photoemission Final-State Effect. *Phys Rev Res* 2024, *6* (4), 043190. https://doi.org/10.1103/PhysRevResearch.6.043190.

(31) Terasawa, T.; Saiki, K. Radiation-Mode Optical Microscopy on the Growth of Graphene. *Nat Commun* 2015, *6* (1), 6834. https://doi.org/10.1038/ncomms7834.

(32) Taira, T.; Obata, S.; Saiki, K. Nucleation Site in CVD Graphene Growth Investigated by Radiation-Mode Optical Microscopy. *Applied Physics Express* 2017, *10* (5), 055502. https://doi.org/10.7567/APEX.10.055502.

(33) Mizuno, S.; Ohta, A.; Suzuki, T.; Kageshima, H.; Yuhara, J.; Hibino, H. Correlation between Structures and Vibration Properties of Germanene Grown by Ge Segregation. *Applied Physics Express* 2021, *14* (12), 125501. https://doi.org/10.35848/1882-0786/ac3185.

(34) Göthelid, M.; Grehk, T. M.; Hammar, M.; Karlsson, U. O.; Flodström, S. A. Adatom and Rest-Atom Contributions in Ge(111) c (2×8) and Ge(111)-Sn(7×7) Core-Level Spectra. *Phys Rev B* 1993, *48* (3), 2012–2015. https://doi.org/10.1103/PhysRevB.48.2012.

(35) Yeh, J. J.; Lindau, I. Atomic Subshell Photoionization Cross Sections and Asymmetry Parameters: $1 \leqslant Z \leqslant 103$. *At Data Nucl Data Tables* 1985, *32* (1), 1–155. https://doi.org/10.1016/0092-640X(85)90016-6.

(36) Tanuma, S.; Powell, C. J.; Penn, D. R. Calculations of Electron Inelastic Mean Free Paths. IX. Data for 41 Elemental Solids over the 50 EV to 30 KeV Range. *Surface and Interface Analysis* 2011, *43* (3), 689–713. https://doi.org/10.1002/sia.3522.

(37) Kurosawa, M.; Ohta, A.; Araidai, M.; Zaima, S. Surface-Segregated Si and Ge Ultrathin Films Formed by Ag-Induced Layer Exchange Process. *Jpn J Appl Phys* 2016, *55* (8S1), 08NB07. https://doi.org/10.7567/JJAP.55.08NB07.

(38) Kazemi, H.; Weber, L. Solid Solubility of Germanium in Silver. *Thermochim Acta* 2012, *544*, 57–62. https://doi.org/10.1016/j.tca.2012.06.018.

(39) Sawaya, S.; Goniakowski, J.; Tréglia, G. Ge Deposition on Ag Surfaces: Dependence of the Adsorption Characteristics on the Surface Orientation. *Phys Rev B Condens Matter Mater Phys* 2000, *61* (12), 8469–8474. https://doi.org/10.1103/PhysRevB.61.8469.

(40) Zhang, K.; Bernard, R.; Borensztein, Y.; Cruguel, H.; Prévot, G. Growth of Germanium-Silver Surface Alloys Followed by in Situ Scanning Tunneling Microscopy: Absence of Germanene Formation. *Phys Rev B* 2020, *102* (12), 125418. https://doi.org/10.1103/PhysRevB.102.125418.

(41) Hung, V. Van; Masuda-Jindo, K. Application of Statistical Moment Method to Thermodynamic Properties of Metals at High Pressures. *J Physical Soc Japan* 2000, *69* (7), 2067–2075. https://doi.org/10.1143/JPSJ.69.2067.

(42) Huang, L.-F.; Gong, P.-L.; Zeng, Z. Phonon Properties, Thermal Expansion, and Thermomechanics of Silicene and Germanene. *Phys Rev B* 2015, *91* (20), 205433. https://doi.org/10.1103/PhysRevB.91.205433.

(43) Shelton, J. C.; Patil, H. R.; Blakely, J. M. Equilibrium Segregation of Carbon to a Nickel (111) Surface: A Surface Phase Transition. *Surf Sci* 1974, *43* (2), 493–520. https://doi.org/10.1016/0039-6028(74)90272-6.

(44) Hoffman, R. E. Self-Diffusion in Dilute Binary Solid Solutions—III. *Acta Metallurgica* 1958, *6* (2), 95–97. https://doi.org/10.1016/0001-6160(58)90118-4.

(45) Zhu, Y.; Zhang, X. Y.; Zhang, S. H.; Yang, J. K.; Han, C.; Hao, A. M.; Liu, R. P. Ge Adsorption on Ag(111): A Density-Functional Theory Investigation. *Solid State Sci* 2012, *14* (10), 1480–1485. https://doi.org/10.1016/j.solidstatesciences.2012.08.021.

(46) Yuhara, J.; He, B.; Matsunami, N.; Nakatake, M.; Le Lay, G. Graphene's Latest Cousin: Plumbene Epitaxial Growth on a "Nano WaterCube." *Advanced Materials* 2019, *31* (27), 1–6. https://doi.org/10.1002/adma.201901017.

(47) Zhu, F.-F.; Chen, W.-J.; Xu, Y.; Gao, C.-L.; Guan, D.-D.; Liu, C.-H.; Qian, D.; Zhang, S.-C.; Jia, J.-F. Epitaxial Growth of Two-Dimensional Stanene. *Nat Mater* 2015, *14* (10), 1020–1025. https://doi.org/10.1038/nmat4384.

(48) Yuhara, J.; Fujii, Y.; Nishino, K.; Isobe, N.; Nakatake, M.; Xian, L.; Rubio, A.; Le Lay, G. Large Area Planar Stanene Epitaxially Grown on Ag(1 1 1). *2d Mater* 2018, *5* (2), 025002. https://doi.org/10.1088/2053-1583/aa9ea0.

(49) Varykhalov, A.; Sánchez-Barriga, J.; Shikin, A. M.; Biswas, C.; Vescovo, E.; Rybkin, A.; Marchenko, D.; Rader, O. Electronic and Magnetic Properties of Quasifreestanding Graphene on Ni. *Phys Rev Lett* 2008, *101* (15), 157601. https://doi.org/10.1103/PhysRevLett.101.157601.

TOC graphics.